Hydrol. Earth Syst. Sci. Discuss., 9, 6185–6201, 2012
www.hydrol-earth-syst-sci-discuss.net/9/6185/2012/
doi:10.5194/hessd-9-6185-2012

Hydrology and Earth System Sciences Discussions

Technical Note: Downscaling RCM precipitation to the station scale using quantile mapping – a comparison of methods

L. Gudmundsson[1,*], **J. B. Bremnes**[1], **J. E. Haugen**[1], **and T. Engen Skaugen**[1]

[1]The Norwegian Meteorological Institute, Oslo, Norway
[*]now at: Institute for Atmospheric and Climate Science, ETH Zürich, Zürich, Switzerland

Received: 10 April 2012 – Accepted: 3 May 2012 – Published: 15 May 2012

Correspondence to: L. Gudmundsson (lukas.gudmundsson@env.ethz.ch)

Published by Copernicus Publications on behalf of the European Geosciences Union.

Abstract

The impact of climate change on water resources is usually assessed at the local scale. However, regional climate models (RCM) are known to exhibit systematic biases in precipitation. Hence, RCM simulations need to be post-processed in order to produce reliable estimators of local scale climate. A popular post-processing approach is quantile mapping (QM), which is designed to adjust the distribution of modeled data, such that it matches observed climatologies. However, the diversity of suggested QM methods renders the selection of optimal techniques difficult and hence there is a need for clarification. In this paper, QM methods are reviewed and classified into: (1) distribution derived transformations, (2) parametric transformations and (3) nonparametric transformations; each differing with respect to their underlying assumptions. A real world application, using observations of 82 precipitation stations in Norway, showed that nonparametric transformations have the highest skill in systematically reducing biases in RCM precipitation.

1 Introduction

It is well established that precipitation simulations from regional climate models (RCM) are biased (e.g. due to limited process understanding or insufficient spatial resolution; Rauscher et al., 2010) and hence need to be post processed (i.e. statistically adjusted, bias corrected) before being used for climate impact assessment (e.g. Christensen et al., 2008; Maraun et al., 2010; Teutschbein and Seibert, 2010; Winkler et al., 2011a,b). In recent years a multitude of studies has investigated different post processing techniques, aiming at providing reliable estimators of observed precipitation climatologies given RCM output (e.g. Ines and Hansen, 2006; Engen-Skaugen, 2007; Schmidli et al., 2007; Dosio and Paruolo, 2011; Themeßl et al., 2011; Turco et al., 2011). Recently, Themeßl et al. (2011) compared several approaches, concluding that quantile mapping (QM) (Panofsky and Brier, 1968) – the mapping of the modeled cumulative distribution function (CDF) of the variable of interest onto the observed CDF – was most efficient in removing precipitation biases, also for the extreme part of the distribution. Hence it is not surprising that QM and closely related approaches have become popular to adjust both RCM (e.g. Ashfaq et al., 2010; Dosio and Paruolo, 2011; Themeßl et al., 2011; Sunyer et al., 2012) and global circulation model (GCM) (e.g. Wood et al., 2004; Ines and Hansen, 2006; Boé et al., 2007; Li et al., 2010; Piani et al., 2010a,b) precipitation. However, there is no general agreement on the optimal technique to solve the QM task and the approaches employed differ at times substantially. Therefore, there is an urgent need for clarifying the relation among different approaches as well as for an objective assessment of their performance.

2 Methods for quantile mapping

Quantile mapping (also referred to as quantile matching, cumulative distribution function matching, quantile-quantile transformation) attempts to find a transformation,

$$P_o = h(P_m), \tag{1}$$

of a modeled variable P_m such that its new distribution equals the distribution of the observed variable P_o. In the context of this paper P_o and P_m denote observed and modeled precipitation respectively. QM is an application of the probability integral transform (Angus, 1994) and if the distribution of the variable of interest is known, the transformation h is defined as

$$P_o = F_o^{-1}(F_m(P_m)), \tag{2}$$

where F_m is the CDF of P_m and F_o^{-1} is the inverse CDF (or quantile function) corresponding to P_o.

Figure 1 illustrates QM using observed and modeled daily precipitation rates from Geiranger, in the fjords of western Norway. Modeled precipitation was extracted from

a HIRHAM RCM simulation with 25 km resolution (Førland et al., 2009, 2011) forced with the ERA40 re-analysis (Uppala et al., 2005) on a model domain covering Norway and the Nordic Arctic. The left panel shows the quantile-quantile plot of observed and modeled precipitation as well as the best fit of an arbitrary function used to approximate the transformation h. The right panel shows the corresponding empirical CDF of observed and modeled values as well as the transformed modeled values. The practical challenge is to find a suitable approximation for the transformation h and different approaches have been suggested in the literature.

2.1 Distribution derived transformations

Quantile mapping can be achieved by using theoretical distributions to solve Eq. (2). This approach has seen wide application for adjusting modeled precipitation (e.g. Ines and Hansen, 2006; Li et al., 2010; Piani et al., 2010a). All these studies assume that F is a mixture of the Bernoulli and the Gamma distribution, where the Bernoulli distribution is used to model the probability of precipitation occurrence and the Gamma distribution used to model precipitation intensities (e.g. Thom, 1968; Mooley, 1973; Cannon, 2008). In this study, further mixtures, i.e. the Bernoulli-Weibull, the Bernoulli-Lognormal and the Bernoulli-Exponential distributions (Cannon, 2012), are also assessed. The parameters of the distributions are estimated by maximum likelihood methods for both P_o and P_m.

2.2 Parametric transformations

The quantile-quantile relation (Fig. 1) can be modeled directly using parametric transformations. Here the suitability of the following parametric transformations for was explored:

$$\hat{P}_o = bP_m \quad (3)$$

$$\hat{P}_o = a + bP_m \quad (4)$$

$$\hat{P}_o = bP_m^c \quad (5)$$

$$\hat{P}_o = b(P_m - x)^c \quad (6)$$

$$\hat{P}_o = (a + bP_m)\left(1 - e^{-(P_m - x)/\tau}\right) \quad (7)$$

where, $\hat{P}_o$ indicates the best estimate of P_o. The simple scaling (Eq. 3) is regularly used to adjust precipitation from RCM (see Maraun et al., 2010, and references therein) and closely related to local intensity scaling (Schmidli et al., 2006; Widmann et al., 2003). The transformations Eq. (4) to Eq. (7) were all used by Piani et al. (2010b) and have been further explored by Dosio and Paruolo (2011).

Following Piani et al. (2010b), all parametric transformations were fitted to the fraction of the CDF corresponding to observed wet days ($P_o > 0$) by minimizing the residual sum of squares. Modeled values corresponding to the dry part of the observed empirical CDF were set to zero.

2.3 Nonparametric transformations

2.3.1 Empirical quantiles (QUANT)

A common approach to QM is to solve Eq. (2) using the empirical CDF of observed and modeled values in stead of assuming parametric distributions (e.g. Wood et al., 2004; Reichle and Koster, 2004; Boé et al., 2007; Themeßl et al., 2011, 2012). Following the procedure of Boé et al. (2007), the empirical CDFs are approximated using tables of the empirical percentiles. Values in between the percentiles are approximated using linear interpolation. If new model values (e.g. from climate projections) are larger than the training values used to estimate the empirical CDF, the correction found for the highest quantile of the training period is used (Boé et al., 2007; Themeßl et al., 2012).

2.3.2 Smoothing-splines (SSPLIN)

The transformation (Eq. 1) can also be modeled using nonparametric regression. We suggest to use cubic smoothing-splines (e.g. Hastie et al., 2001), although other nonparametric methods may be equally efficient. Like for the parametric transformations (Sect. 2.2) the smoothing spline is only fitted to the fraction of the CDF corresponding to observed wet days and modeled values below this are set to zero. The smoothing parameter of the spline is identified by means of generalized cross-validation.

3 Performance of quantile mapping

3.1 Data and implementation

The suitability of the different QM methods to correct model precipitation from the HIRHAM RCM forced with the ERA40 re-analysis was tested using observed daily precipitation rates of 82 stations in Norway, all covering the 1960–2000 time interval. The QM methods where implemented in the R language (R Development Core Team, 2011) and bundled in the package "qmap" which is made available on the Comprehensive R Archive Network (http://www.cran.r-project.org/).

3.2 Skill scores

To assess the performance of different QM methods a set of scores is needed that quantifies the similarity of the observed and the (corrected) modeled empirical CDF. Previously used scores include overall measures such as the root mean square error (Piani et al., 2010b) and the Kolmogorov-Smirnov two sample statistic (Dosio and Paruolo, 2011). Other suggested scores assess specific moments of the distribution including the mean (Engen-Skaugen, 2007; Li et al., 2010; Dosio and Paruolo, 2011; Themeßl et al., 2011; Turco et al., 2011), the standard deviation (Engen-Skaugen, 2007; Li et al., 2010; Themeßl et al., 2011) and the skewness (Li et al., 2010). A variety of further scores are based on the comparing of the frequency of days with precipitation (Schmidli et al., 2006, 2007; Themeßl et al., 2011) and the magnitude of selected (mostly high) percentiles (Schmidli et al., 2006, 2007; Li et al., 2010; Themeßl et al., 2011). All these scores are either presented as maps or as spatial averages which facilitate a quantitative comparison of methods. One limitation of the scores above is that they can often not be summarized into one global measure; e.g. due to different physical units or lack of normalization. This renders a global evaluation, combining the advantages and drawbacks of different QM methods difficult. Therefore, this study suggests a novel set of scores, aiming at a global evaluation, while keeping track of many relevant properties of the distribution. Overall performance is measured using the mean absolute error (MAE) between the observed and the corrected empirical CDF. To assess the performance for more specific properties related, for example, to the fraction of dry days, average intensities or precipitation extremes other scores are required. Here these properties are assessed using $MAE_{0.1}$, $MAE_{0.2}$, ..., $MAE_{1.0}$, mean absolute errors computed for equally spaced probability intervals of the observed empirical CDF. The subscript indicates the upper bounds of 0.1 wide probability intervals. $MAE_{0.1}$, for example, evaluates differences in the dry part of the distribution, indicating discrepancies in the number of wet days. Similarly, $MAE_{1.0}$ indicates differences in the magnitude of the most extreme events. Note also that MAE can be computed as the mean of $MAE_{0.1}$, $MAE_{0.2}$, $\ldots$, $MAE_{1.0}$, which demonstrates the consistency of these measures. To reduce the risk of over fitting all scores were estimated using a 10-fold cross-validation (CV) (e.g. Hastie et al., 2001) and the mean CV error is reported.

Figure 2 shows the MAE for all stations and all methods under consideration. For the uncorrected model output MAE has pronounced geographic variations. The largest errors are found along the west coast, where the model cannot resolve the orographic effect on precipitation with sufficient detail. Most QM methods reduce the error and even out some of its spatial variability. An exception is the transformation based on the Bernoulli-Log-normal distribution, which does not lead to any visible improvements.

The largest improvements are achieved by parametric and nonparametric transformations, especially along the west coast.

Figure 3 shows the total MAE and $MAE_{0.1}$, $MAE_{0.2}$, ..., $MAE_{1.0}$ averaged over all stations. Most QM methods reduce both the total MAE as well as the MAE for the percentile intervals. The absolute improvements are in most cases largest for the upper part of the CDF ($p \geq 0.5$). Note however, that two of the distribution derived transformations (Bernoulli-Exponential and Bernoulli-Log-normal) increase the error for the most extreme values. In the lower part of the CDF the absolute improvements are generally smaller, owing to the small (often zero) precipitation rates.

3.3 Ranking of methods

In order to obtain a global comparison of the efficiency of the different methods their performance was ranked, closely following the procedure suggested by Reichler and Kim (2008). In a first step, relative errors are computed for each method by dividing the spatial averages of MAE and $MAE_{0.1}$, $MAE_{0.2}$, ..., $MAE_{1.0}$ by the corresponding scores of the uncorrected model output. In other words, the relative errors are defined as the individual points in Fig. 3 divided by the solid line. The relative errors range from an optimal value of zero to infinity. A value smaller than one indicates that the QM method causes an improvement; larger values indicate worsening. The relative errors where finally averaged for each method and ordered from the lowest (best method) to the highest value (worst method).

Figure 4 shows the ranking of the methods, based on the mean of the relative error (black dots). The hollow symbols show the relative errors for the total MAE and the MAE for all percentile intervals. The two nonparametric methods SSPLINE and QUANT have on average the best skill in reducing systematic errors, also for very high (extreme) quantiles. The success of the nonparametric transformations is likely related their flexibility as they do not relying on any predetermined function. This flexibility allows good fits to any quantile-quantile relation. For all highly adaptable methods with many degrees of freedom, over fitting may be a concern. Recall, however, that all scores are estimated using a 10-fold CV, which reduces the risk of over fitting effectively. Nevertheless, over fitting may be an issue if QM methods are fitted to small data samples, i.e distributions of time series that cover only a short period of time. The large spread in performance of parametric transformations is likely related to the flexibility of the different functions. Parametric transformations with three or more free parameters (Eqs. 6 and 7) are almost as efficient as their nonparametric counterparts. Transformations with less flexibility, in particular the simple scaling function (Eq. 3), do have worse performance. The distribution derived transformations rank on average lowest. The best ranking distribution derived transformation is based on the Bernoulli-Weibull distribution. The transformation derived from the Bernoulli-Log-normal distribution has the lowest performance of all considered methods. Note also that all distribution derived transformations have particularly low performance with respect to the extreme part of the distribution. The low performance of distribution derived transformation may seem somewhat surprising, given the theoretical elegance of this approach. This is likely related to the fact that the parameters of the distributions are identified for P_o and P_m separately, which does not guarantee an optimal transformation (Eq. 1).

4 Conclusions

The three approaches to QM assessed in this paper differ substantially with respect to their underlying assumptions, despite the fact that they are all designed to transform RCM output such that its empirical distribution matches the distribution of observed values. A real-world evaluation of a wide range of QM methods showed that most of them are capable to remove biases in RCM precipitation. Despite this overall success, it was also demonstrated that the performance of the QM methods differ substantially. Therefore we stress that QM methods should not be applied without checking their suitability for the data under consideration. The methods with the best skill in reducing biases from RCM precipitation through the entire range of the distribution are all classified as nonparametric transformations. These have the additional advantage that

they can be applied without specific assumptions and are thus recommended for most applications of statistical bias correction.

Acknowledgements. This research was co-funded by the MIST project, a collaboration between the hydro-power company Statkraft and the Norwegian Meteorological Institute.

References

Angus, J. E.: The Probability Integral Transform and Related Results, SIAM Rev., 36, 652–654, 1994. 6187

Ashfaq, M., Bowling, L. C., Cherkauer, K., Pal, J. S., and Diffenbaugh, N. S.: Influence of climate model biases and daily-scale temperature and precipitation events on hydrological impacts assessment: A case study of the United States, J. Geophys. Res., 115, D14116, doi:10.1029/2009JD012965, 2010. 6187

Boé, J., Terray, L., Habets, F., and Martin, E.: Statistical and dynamical downscaling of the Seine basin climate for hydro-meteorological studies, Int. J. Climatol., 27, 1643–1655, doi:10.1002/joc.1602, 2007. 6187, 6189

Cannon, A. J.: Probabilistic Multisite Precipitation Downscaling by an Expanded Bernoulli-Gamma Density Network, J. Hydrometeorol., 9, 1284–1300, doi:10.1175/2008JHM960.1, 2008. 6188

Cannon, A. J.: Neural networks for probabilistic environmental prediction: Conditional Density Estimation Network Creation and Evaluation (CaDENCE) in R, Comput. Geosci., 41, 126 – 135, doi:10.1016/j.cageo.2011.08.023, 2012. 6188

Christensen, J. H., Boberg, F., Christensen, O. B., and Lucas-Picher, P.: On the need for bias correction of regional climate change projections of temperature and precipitation, Geophys. Res. Lett., 35, L20709, doi:10.1029/2008GL035694, 2008. 6186

Dosio, A. and Paruolo, P.: Bias correction of the ENSEMBLES high-resolution climate change projections for use by impact models: Evaluation on the present climate, J. Geophys. Res., 116, D16106, doi:10.1029/2011JD015934, 2011. 6186, 6187, 6189, 6190

Engen-Skaugen, T.: Refinement of dynamically downscaled precipitation and temperature scenarios, Climatic Change, 84, 365–382, doi:10.1007/s10584-007-9251-6, 2007. 6186, 6190

Førland, E. J., Benestad, R. E., Flatø, F., Hanssen-Bauer, I., Haugen, J. E., Isaksen, K., Sorteberg, A., and Ådlandsvik, B.: Climate development in North Norway and the Svalbard region during 1900–2100, Tech. Rep. 128, Norwegian Polar Institute, available at: http://www.npolar.no (last access: 15 May 2012), 2009. 6188

Førland, E. J., Benestad, R., Hanssen-Bauer, I., Haugen, J. E., and Skaugen, T. E.: Temperature and Precipitation Development at Svalbard 1900–2100, Adv. Meteorol., 2011, 893790, doi:10.1155/2011/893790, 2011. 6188

Hastie, T., Tibshirani, R., and Friedman, J. H.: The Elements of Statistical Learning, Springer, 2001. 6190, 6191

Ines, A. V. and Hansen, J. W.: Bias correction of daily GCM rainfall for crop simulation studies, Agr. Forest Meteorol., 138, 44–53, doi:10.1016/j.agrformet.2006.03.009, 2006. 6186, 6187, 6188

Li, H., Sheffield, J., and Wood, E. F.: Bias correction of monthly precipitation and temperature fields from Intergovernmental Panel on Climate Change AR4 models using equidistant quantile matching, J. Geophys. Res., 115, D10101, doi:10.1029/2009JD012882, 2010. 6187, 6188, 6190, 6191

Maraun, D., Wetterhall, F., Ireson, A. M., Chandler, R. E., Kendon, E. J., Widmann, M., Brienen, S., Rust, H. W., Sauter, T., Themeßl, M., Venema, V. K. C., Chun, K. P., Goodess, C. M., Jones, R. G., Onof, C., Vrac, M., and Thiele-Eich, I.: Precipitation downscaling under climate change: Recent developments to bridge the gap between dynamical models and the end user, Rev. Geophys., 48, RG3003, doi:10.1029/2009RG000314, 2010. 6186, 6189

Mooley, D. A.: Gamma Distribution Probability Model for Asian Summer Monsoon Monthly Rainfall, Mon. Weather Rev., 101, 160–176, doi:10.1175/1520-0493(1973)101¡0160:GDPMFA¿2.3.CO;2, 1973. 6188

Panofsky, H. W. and Brier, G. W.: Some Applications of Statistics to Meteorology, The Pennsylvania State University Press, Philadelphia, 1968. 6186

Piani, C., Haerter, J., and Coppola, E.: Statistical bias correction for daily precipitation in regional climate models over Europe, Theor. Appl. Climatol., 99, 187–192, doi:10.1007/s00704-009-0134-9, 2010a. 6187, 6188

Piani, C., Weedon, G., Best, M., Gomes, S., Viterbo, P., Hagemann, S., and Haerter, J.: Statistical bias correction of global simulated daily precipitation and temperature for the application of hydrological models, J. Hydrol., 395, 199–215, doi:10.1016/j.jhydrol.2010.10.024, 2010b. 6187, 6189, 6190

R Development Core Team: R: A Language and Environment for Statistical Computing, R Foundation for Statistical Computing, Vienna, Austria, http://www.R-project.org/ (last access: 15 May 2012), 2011. 6190

Rauscher, S., Coppola, E., Piani, C., and Giorgi, F.: Resolution effects on regional climate model simulations of seasonal precipitation over Europe, Clim. Dynam., 35, 685–711, doi:10.1007/s00382-009-0607-7, 2010. 6186

Reichle, R. H. and Koster, R. D.: Bias reduction in short records of satellite soil moisture, Geophys. Res. Lett., 31, L19501, doi:10.1029/2004GL020938, 2004. 6189

Reichler, T. and Kim, J.: How Well Do Coupled Models Simulate Today's Climate?, B. Am. Meteorol. Soc., 89, 303–311, doi:10.1175/BAMS-89-3-303, 2008. 6192

Schmidli, J., Frei, C., and Vidale, P. L.: Downscaling from GCM precipitation: a benchmark for dynamical and statistical downscaling methods, Int. J. Climatol., 26, 679–689, doi:10.1002/joc.1287, 2006. 6189, 6191

Schmidli, J., Goodess, C. M., Frei, C., Haylock, M. R., Hundecha, Y., Ribalaygua, J., and Schmith, T.: Statistical and dynamical downscaling of precipitation: An evaluation and comparison of scenarios for the European Alps, J. Geophys. Res., 112, D04105, doi:10.1029/2005JD007026, 2007. 6186, 6191

Sunyer, M., Madsen, H., and Ang, P.: A comparison of different regional climate models and statistical downscaling methods for extreme rainfall estimation under climate change, Atmos. Res., 103, 119–128, doi:10.1016/j.atmosres.2011.06.011, 2012. 6187

Teutschbein, C. and Seibert, J.: Regional Climate Models for Hydrological Impact Studies at the Catchment Scale: A Review of Recent Modeling Strategies, Geogr. Compass, 4, 834–860, doi:10.1111/j.1749-8198.2010.00357.x, 2010. 6186

Themeßl, M. J., Gobiet, A., and Leuprecht, A.: Empirical-statistical downscaling and error correction of daily precipitation from regional climate models, Int. J. Climatol., 31, 1530–1544, doi:10.1002/joc.2168, 2011. 6186, 6187, 6189, 6190, 6191

Themeßl, M. J., Gobiet, A., and Heinrich, G.: Empirical-statistical downscaling and error correction of regional climate models and its impact on the climate change signal, Climatic Change, 112, 449–468, doi:10.1007/s10584-011-0224-4, 2012. 6189

Thom, H. C. S.: Approximate convolution of the gamma and mixed gamma distributions, Mon. Weather Rev., 96, 883–886, doi:10.1175/1520-0493(1968)096¡0883:ACOTGA¿2.0.CO;2, 1968. 6188

Turco, M., Quintana-Seguí, P., Llasat, M. C., Herrera, S., and Gutiérrez, J. M.: Testing MOS precipitation downscaling for ENSEMBLES regional climate models over Spain, J. Geophys. Res., 116, D18109, doi:10.1029/2011JD016166, 2011. 6186, 6190

Uppala, S. M., Kållberg, P. W., Simmons, A. J., Andrae, U., Bechtold, V. D. C., Fiorino, M., Gibson, J. K., Haseler, J., Hernandez, A., Kelly, G. A., Li, X., Onogi, K., Saarinen, S., Sokka, N., Allan, R. P., Andersson, E., Arpe, K., Balmaseda, M. A., Beljaars, A. C. M., Berg, L. V. D., Bidlot, J., Bormann, N., Caires, S., Chevallier, F., Dethof, A., Dragosavac, M., Fisher, M., Fuentes, M., Hagemann, S., Hólm, E., Hoskins, B. J., Isaksen, L., Janssen, P. A. E. M., Jenne, R., Mcnally, A. P., Mahfouf, J.-F., Morcrette, J.-J., Rayner, N. A., Saunders, R. W., Simon, P., Sterl, A., Trenberth, K. E., Untch, A., Vasiljevic, D., Viterbo, P., and Woollen, J.: The ERA-40 re-analysis, Q. J. Roy. Meteorol. Soc., 131, 2961–3012, doi:10.1256/qj.04.176, 2005. 6188

Widmann, M., Bretherton, C. S., and Salathé, E. P.: Statistical Precipitation Downscaling over the Northwestern United States Using Numerically Simulated Precipitation as a Predictor, J. Climate, 16, 799–816, doi:10.1175/1520-0442(2003)016¡0799:SPDOTN¿2.0.CO;2, 2003. 6189

Winkler, J. A., Guentchev, G. S., Liszewska, M., Perdinan, and Tan, P.-N.: Climate Scenario Development and Applications for Local/Regional Climate Change Impact Assessments: An Overview for the Non-Climate Scientist – Part II: Considerations When Using Climate Change Scenarios, Geogr. Compass, 5, 301–328, doi:10.1111/j.1749-8198.2011.00426.x, 2011a. 6186

Winkler, J. A., Guentchev, G. S., Perdinan, Tan, P.-N., Zhong, S., Liszewska, M., Abraham, Z., Niedźwiedź, T., and Ustrnul, Z.: Climate Scenario Development and Applications for Local/Regional Climate Change Impact Assessments: An Overview for the Non-Climate Scientist – Part I: Scenario Development Using Downscaling Methods, Geogr. Compass, 5, 275–300, doi:10.1111/j.1749-8198.2011.00425.x, 2011b. 6186

Wood, A. W., Leung, L. R., Sridhar, V., and Lettenmaier, D. P.: Hydrologic Implications of Dynamical and Statistical Approaches to Downscaling Climate Model Outputs, Climatic Change, 62, 189–216, doi:10.1023/B:CLIM.0000013685.99609.9e, 2004. 6187, 6189

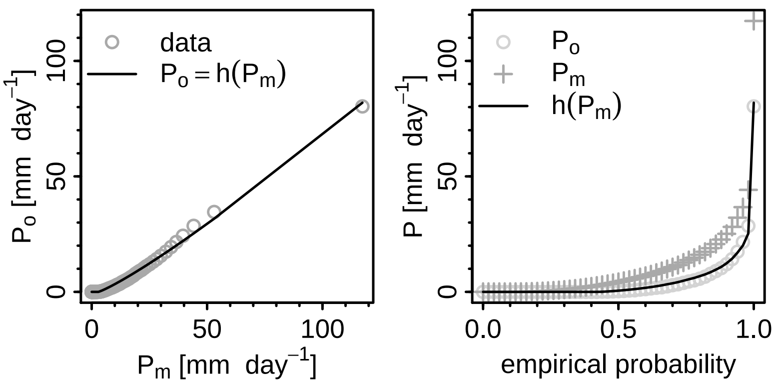

Fig. 1. Left panel: quantile-quantile plot of observed (P_o) and modeled (P_m) precipitation in Geiranger, Norway, as well as a transformation ($P_o = h(P_m)$) that is used to map the modeled onto observed quantiles. Right panel: empirical CDF of observed, modeled and transformed ($h(P_m)$) precipitation.

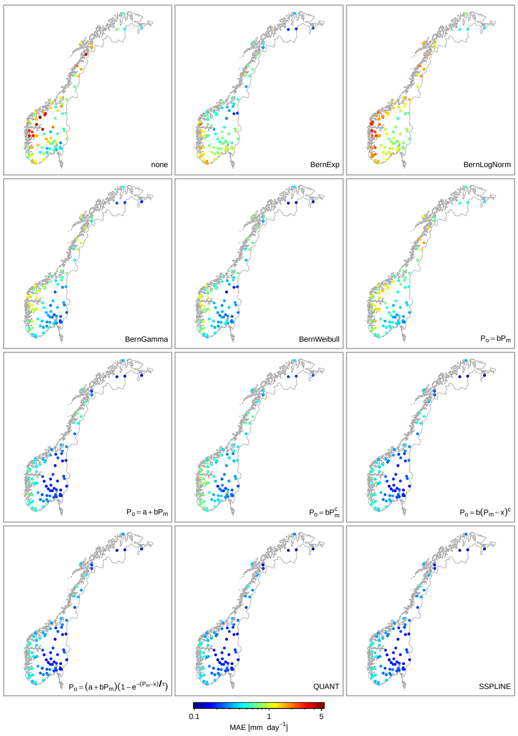

Fig. 2. Mean Absolute Error (MAE) between the observed and modeled empirical CDF for different QM methods. "none" indicates uncorrected modeled values. Equations: parametric transformations. Distribution derived transformations are based on the Bernoulli-Exponential (BernExp), the Bernoulli-Log-normal (BernLogNorm), the Bernoulli-Gamma (BernGamma) and the Bernoulli-Weibull (BernWeibull) distributions. QUANT: QM based on empirical quantiles. SSPLINE: QM using a smoothing-spline.

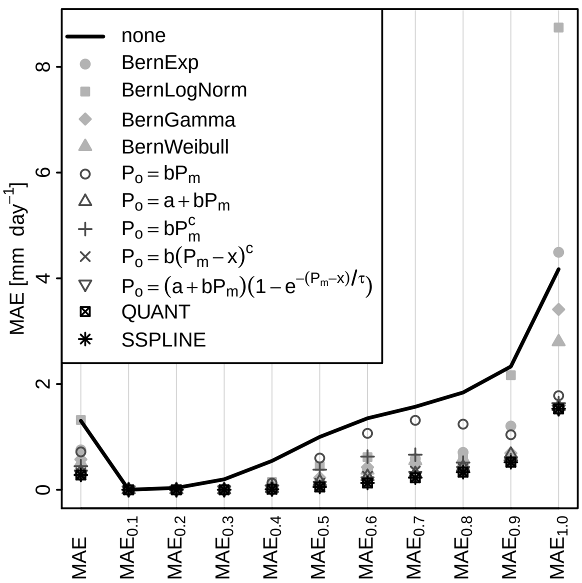

Fig. 3. Total Mean Absolute Error (MAE) and the mean absolute error for specific probability intervals ($MAE_{0.1}$, $MAE_{0.2}$, ..., $MAE_{1.0}$), averaged over all stations.

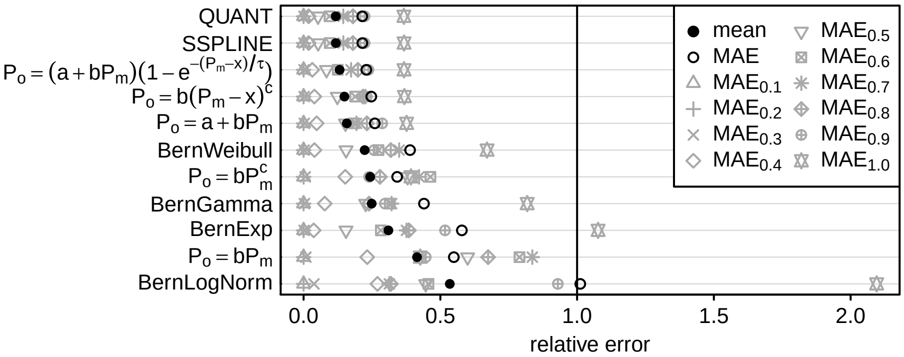

Fig. 4. Total Mean Absolute Error (MAE) and the mean absolute error for specific probability intervals ($MAE_{0.1}$, $MAE_{0.2}$, ..., $MAE_{1.0}$), averaged over all stations.